DOI: 10.15669/pnst.8.64

Progress in Nuclear Science and Technology
Volume 8 (2025) pp. 64-69

ARTICLE

Preparation of Feedstock for Uranium and Plutonium Mixed Oxide Fuels Containing Minor Actinides by Microwave Heating

Masaumi NAKAHARA [1*], Tatsuya SENZAKI [1], Yuichi SANO [1] and Masato KATO [2]

[1] *Japan Atomic Energy Agency, 4-33 Muramatsu, Tokai-mura, Naka-gun, Ibaraki-ken 319-1194, Japan*
[2] *Inspection Development Company Ltd., 4-33 Muramatsu, Tokai-mura, Naka-gun, Ibaraki-ken 319-1112, Japan*

To prepare a feedstock of U and Pu mixed oxide (MOX) fuel powder containing minor actinides (MA), MA was recovered from high-level liquid waste derived from irradiated fast reactor fuel using extraction chromatography. The recovered MA nitrate solution was then mixed with U and Pu nitrate solution, and MOX fuel powders containing MA were prepared using microwave heating. In addition to these powders, another MOX fuel powder was prepared without adding the MA nitrate solution. Both samples were characterized using X-ray diffraction (XRD) analysis. The XRD results revealed differences in the MOX fuel powders prepared with and without adding MA nitrate solution. These differences are attributed to the presence of U hydroxides in both types of MOX fuel powders. Overall, this study provides basic experimental data on the denitration behavior and characteristics of MA-bearing MOX fuel powders. Further investigation is needed to better understand these processes, and denitration conditions need to be optimized for the efficient preparation of MA-bearing MOX fuel powders.

KEYWORDS: microwave heating, mixed oxide fuel, uranium, plutonium, minor actinides

I. Introduction

In Japan, U and Pu recovered from irradiated fast reactor fuel are proposed to load a fast reactor as nuclear fuel in the fast reactor fuel cycle. To reduce the radiotoxic potential and volume of high-level radioactive waste derived from irradiated fast reactor fuel, minor actinides (MA) such as Np, Am, and Cm are also recovered from high-level liquid waste and repurposed as fast reactor fuel.[1)] Within the fast reactor fuel cycle, MA is burnt in the fast reactor, preventing any increase in their overall quantity. The fast reactor fuel cycle enables the use of low decontamination U and Pu mixed oxide (MOX) fuel containing MA, enabling simplifications in the reprocessing procedure. These advancements are expected to enhance economic competitiveness and improve nuclear proliferation resistance.

To support the development of the fast reactor fuel cycle, the Japan Atomic Energy Agency (JAEA) has undertaken six key research and development initiatives: (1) preparation of feedstock for MA-bearing MOX fuel powders, (2) development of remote fuel fabrication technology, (3) establishment of a database for the characterization and design of MOX fuel containing MA, (4) development of analysis technologies for MOX fuel and behavior characterization of nuclear transmutation, (5) development of post-irradiation examination, and (6) execution of transient radiation experiments with the Transient Reactor Test Facility.[2)]

As part of the first initiative, the JAEA plans to adjust the Pu content in MOX fuel powders by mixing nitrate solutions before denitration and conversion. Subsequently, it plans to demonstrate the preparation of MOX fuel powder using a microwave heating method.[3)] This approach would eliminate the need for the weighing and mixing processes during fuel fabrication, thereby simplifying the nuclear fuel fabrication process. Additionally, the formation of Pu and MA spots in MOX pellets could be avoided.

The JAEA has already developed the microwave heating method to enhance nuclear nonproliferation. In this method, a Pu nitrate solution is mixed with a U nitrate solution, and H_2O and HNO_3 from these nitrate solutions are vaporized using microwaves. Unlike the oxalic acid precipitation method,[4)] which involves precipitation and filtration processes, the microwave heating method directly denitrates the mixed U and Pu nitrate solution. This approach helps reduce the volume of radioactive liquid waste. Furthermore, it offers an advantage in fuel fabrication as U and Pu are homogeneously mixed in a fluid state, thus preventing the Pu spots in the MOX fuel.

Researchers worldwide have studied the fabrication and characterization of MA-bearing MOX fuel.[5-7)] The irradiation behavior of this fuel in fast reactors has also been investigated.[8-10)] Notably, the denitration behavior and characteristics of MA-bearing MOX fuel powders are complex, making it essential to evaluate these aspects. The study of the denitration behavior and characteristics of MA-bearing MOX fuel powders recovered from irradiated fast reactor MOX fuel provides valuable experimental data for this initiative.

This paper reports on the preparation of feedstock for MA-bearing MOX fuel powders and their analysis. During the preparation process, MA was recovered from the raffinate of solvent extraction using an extraction

*Corresponding author, E-mail: nakahara.masaumi@jaea.go.jp

chromatography process and then mixed with the U and Pu nitrate solution. To confirm the influence of MA in the MOX fuel powders, a preparation experiment was conducted by denitrating only the U and Pu nitrate solution without adding the MA nitrate solution. The microwave heating method was applied to denitrate and convert these solutions into MA-bearing MOX fuel powders. Examining the denitration behavior and characteristics of MA-bearing MOX fuel powders offers valuable insights for fuel fabrication and the comprehension of irradiation behavior. Therefore, the MA-bearing MOX fuel powders were analyzed using X-ray diffraction (XRD) and thermogravimetry-differential thermal analysis (TG-DTA). The preparation and analysis were performed at the Chemical Processing Facility (CPF) of the JAEA.

II. Experimental

1. Materials and Procedure

Irradiated fuel pins from fast reactor Joyo Mk-II and Mk-IIC were used for advanced reprocessing experiments within the fast reactor fuel cycle. The Mk-II fuel pins had an average burnup of 63.7 GWd t^{-1} and a cooling time of approximately 26 years, while the Mk-IIC fuel pins had an average burnup of 99.8 GWd t^{-1} and a cooling time of approximately 23 years.[11] The fuel pins were cut and dissolved in HNO_3 solutions within a hot cell at the CPF. Among the actinides in the dissolver solution of the irradiated fast reactor fuel, U, Pu, and Np were recovered through a solvent extraction process.[11]

On the other hand, MA in the raffinate derived from the solvent extraction process was recovered using an extraction chromatography process. In the separation process, styrene-divinylbenzene copolymer-coated porous SiO_2 particles impregnated with an extractant were used as adsorbents. The raffinate was passed through a column of *n*-octyl(phenyl)-*N,N*-diisobutylcarbamoylmethylphosphine oxide (CMPO).[12] Then, MA and lanthanides in the raffinate are separated from fission products (FP) using a solution containing diethylenetriamine-*N,N,N',N'',N''*-pentaacetic acid (DTPA). The H^+ concentration in the product obtained from the CMPO column was adjusted to 0.3 mol dm^{-3}, and the nitrate solution was fed to a column containing bis(2-ethylhexyl) hydrogen phosphate (HDEHP).[13] Am and Cm were separated from lanthanides with a 0.8 mol dm^{-3} HNO_3 stripping solution.

The MA nitrate solution was transferred from the hot cell to a glove box for denitration and conversion to oxide powders. Subsequently, this solution was mixed with the U and Pu nitrate solution, prepared by dissolving unirradiated MOX fuel pellets. This mixed nitrate solution was poured into a Si_3N_4 denitration dish and treated in a microwave oven. The nitrate solution was concentrated at approximately 200°C. In particular, the microwave oven was pre-heated at 200°C, and the concentrated solution in the rotating denitration dish was exposed to microwaves for 30 min at 1500 W. Subsequently, the solution was heated at 750°C for 10 min in air. After cooling, the resulting MOX fuel powder containing MA was recovered. For comparative evaluation, MOX fuel powder was also prepared without adding the MA nitrate solution. The structural and thermal properties of both types of MOX fuel powders were evaluated to assess their characteristics.

2. Analysis

The H^+ concentration in the solutions was measured using a titrator (COM-2500, Hiranuma Sangyo Co., Ltd.). Meanwhile, the U and Pu concentrations were measured by colorimetry (V-570, JASCO Corporation), and other metal concentrations were quantified by inductively coupled plasma atomic emission spectrometry (ICP-AES; ICPS-7510, Shimadzu Corporation). Radioactive concentrations were evaluated by alpha-ray spectrometry (detector: CU-017-450-100 and pulse height analyzer: 920E, ORTEC) and gamma-ray spectrometry (detector: GEM-10 and pulse height analyzer: 92X MCA, ORTEC). The morphology of the MOX fuel powders was examined using a scanning electron microscope (SEM; Mighty-8DX, Technex Lab Co., Ltd.) within the glove box. The structural properties of the MA-bearing MOX fuel powders were analyzed using XRD equipment (RINT-2100H/PC, Rigaku Corporation) equipped with a CuKα radiation source at a scan speed of 5° min^{-1}. The XRD voltage and current were 20 kV and 20 mA, respectively. Thermal properties were assessed by TG-DTA (DTG-50, Shimadzu Corporation) under an Ar atmosphere within a glove box. During TG-DTA, the samples were heated at a rate of 10°C min^{-1}.

III. Results and Discussion

1. Preparation of Mixed Oxide Fuel Powders Containing Minor Actinides

MA in the raffinate was recovered using extraction chromatography with CMPO and HDEHP columns. In the first step, MA and lanthanides were stripped from the CMPO column using a 0.05 mol dm^{-3} DTPA solution. Most of the Am was collected in the product containing DTPA. According to the elution sequence, Am was separated from Eu in the HDEHP column using the 0.8 mol dm^{-3} HNO_3 solution. While a portion of Am accumulated in the column, sufficient amounts of MA were successfully eluted.

Table 1 Concentrations of elements in the MA nitrate solution

Element	Concentration (g dm^{-3})	Element	Concentration (g dm^{-3})
B	$< 1.5 \times 10^{-2}$	Mo	$< 1.5 \times 10^{-2}$
Na	1.3×10^{-2}	Ru	$< 1.0 \times 10^{-2}$
Al	$< 1.5 \times 10^{-2}$	Rh	$< 5.0 \times 10^{-3}$
Si	$< 2.0 \times 10^{-2}$	Pd	$< 1.0 \times 10^{-2}$
Ca	$< 1.5 \times 10^{-2}$	Ba	$< 5.0 \times 10^{-3}$
Cr	$< 5.0 \times 10^{-3}$	La	$< 1.5 \times 10^{-2}$
Fe	$< 1.0 \times 10^{-2}$	Ce	$< 1.5 \times 10^{-2}$
Ni	$< 5.0 \times 10^{-3}$	Pr	$< 5.0 \times 10^{-3}$
Zn	$< 7.5 \times 10^{-2}$	Nd	3.9×10^{-2}
Sr	$< 5.0 \times 10^{-3}$	Sm	$< 5.0 \times 10^{-3}$
Y	$< 5.0 \times 10^{-3}$	Eu	$< 5.0 \times 10^{-3}$
Zr	$< 1.5 \times 10^{-2}$		

Table 2 Concentrations of nuclides in the MA nitrate solution

Nuclide	Concentration (Bq cm^{-3})	Nuclide	Concentration (Bq cm^{-3})
^{54}Mn	$< 3.7 \times 10^4$	^{137}Cs	$< 3.7 \times 10^4$
^{60}Co	$< 3.7 \times 10^4$	^{144}Ce	$< 3.7 \times 10^4$
^{95}Zr	$< 3.7 \times 10^4$	^{144}Pr	$< 3.7 \times 10^4$
^{95}Nb	$< 3.7 \times 10^4$	^{154}Eu	$< 3.7 \times 10^4$
^{103}Ru	$< 3.7 \times 10^4$	^{155}Eu	$< 3.7 \times 10^4$
^{106}Ru	$< 3.7 \times 10^4$	^{241}Am	1.4×10^7
^{125}Sb	$< 3.7 \times 10^4$	^{242}Cm	3.2×10^5
^{134}Cs	$< 3.7 \times 10^4$	^{244}Cm	4.4×10^5

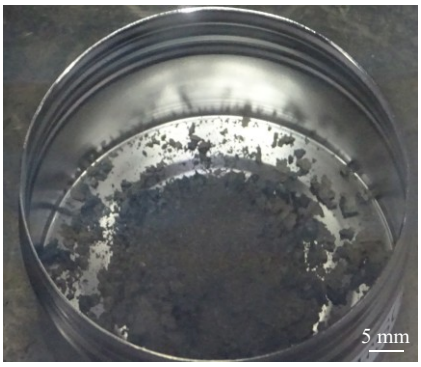

Fig. 1 Appearance of the MA-bearing MOX fuel powder prepared by mixing the MA nitrate solution with the dissolver solution of MOX fuel pellets

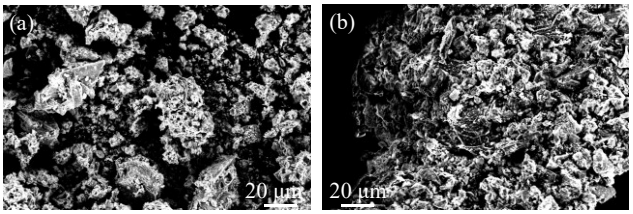

Fig. 2 SEM images of MA-bearing MOX fuel powders: (a) 2.3% MA-bearing MOX fuel powder and (b) 6.8% MA-bearing MOX fuel powder

Table 1 summarizes the element concentrations in the MA nitrate solution before denitration. As indicated, minimal amounts of Na and Nd were detected, while the concentrations of other elements were below the detection limit of ICP-AES. **Table 2** summarizes the nuclide concentrations in the MA nitrate solution before denitration. The data indicate that the radioactivity of all FP in the MA nitrate solution was below the detection limit of gamma-ray spectrometry. The MA content in the MOX fuel powder prepared using mixed nitrate solution, containing the U, Pu, and MA nitrate solutions, was determined to be 6.8%. The weight ratios of U, Pu, Am, and Cm were approximately 6.5×10^{-1}, 2.8×10^{-1}, 6.8×10^{-2}, and 7.1×10^{-5}, respectively. Meanwhile, the MOX fuel powder prepared without adding the MA nitrate solution contained 2.3% of ^{241}Am, which is formed in situ through the decay of ^{241}Pu. The weight ratios of U, Pu, and Am were approximately 6.9×10^{-1}, 2.8×10^{-1}, and 2.3×10^{-2}, respectively.

In this study, MA-bearing MOX fuel powders were prepared using microwave heating. **Figure 1** shows the appearance of the MA-bearing MOX fuel powders recovered from microwave heating equipment. **Figure 2** depicts the SEM images of the MA-bearing MOX fuel powders. No notable differences in appearance were observed between the samples. Both types of MA-bearing MOX fuel powders had particle diameters ranging from 20–500 μm.

2. Evaluation of Mixed Oxide Fuel Powders Containing Minor Actinides

It is reported that UO_2 oxidation exhibits non-stoichiometric phases,[14] which influence its physical properties and neutron irradiation behavior. During oxidation in air, U assumes various valence states, with U_3O_7 and U_4O_9 forming as intermediate oxidation products. In these phases, additional O atoms occupy unoccupied cubic sites in the CaF_2-type lattice structure. During $(U_{0.75}Pu_{0.25})O_2$ oxidation, the M_4O_9 forms directly without the formation of M_3O_7.[15-17] Although UO_2 is oxidized to U_3O_8 in air, MOX fuel does not independently form a M_3O_8 phase. Instead, a mixture of M_3O_8 and M_4O_9 phases is formed.[18] The M_4O_9 phase appears at an O/M ratio of 2.25 in the MOX fuel powder.[16] According to the MO_2–M_4O_9 phase diagram, stable regions of MO_{2+x} and M_4O_{9-y} depend on both temperature and the O/M ratio.[19] However, given the structural similarities between $M_4O_{9\pm y}$ and MO_{2+x}, distinguishing between the two phases is challenging.[20]

The oxidation behavior of MOX fuel containing 30% Pu content was investigated in a 20% O_2 and 80% Ar atmosphere at 100–800°C.[21] The O/M ratios of the MOX fuel increased with rising temperature and declining Pu content at 100–400°C. On the other hand, at 600 and 800°C, the O/M ratios were 2.428 and 2.422, respectively.[21] According to thermodynamic data, the O/M ratio tends to decrease with rising temperature at 1100–1350°C in MO_{2+x},[22] and a similar tendency was confirmed in the experimental results at 600 and 800°C. Oxidation at 800°C confirmed the coexistence of the M_3O_8 and M_4O_{9+y} phases. The XRD pattern of the MOX fuel containing 30% Pu presented the (111) peak of MO_2 at 28.34°. Furthermore, as the value of x in MO_{2+x} increased, the peak shifted to higher angles.[21] Additionally, the M_3O_8 peak appeared in the XRD pattern of MOX fuels containing 30% Pu content with O/M ratios of 2.36–2.43.

The structural properties of MA-bearing MOX fuel powders were measured by XRD. The measured XRD data were analyzed using DIFFRAC.TOPAS, a profile fitting software provided by Bruker AXS GmbH for quantitative phase and crystal structure analyses. **Figure 3** shows the XRD pattern of the 2.3% MA-bearing MOX fuel powder. This powder comprises a MOX lattice (space group Fm3m) with a lattice parameter a = 5.408 Å and an α-$UO_2(OH)_2$ lattice (space group Cmca) with lattice parameters a = 4.295 Å, b = 10.244 Å, and c = 6.943 Å. The aggregate size was estimated to be 20–50 nm. **Figure 4** shows the XRD pattern of the 6.8% MA-bearing MOX fuel powder. This powder comprises a MOX lattice (space group Fm3m) with a lattice parameter a = 5.405 Å and a $(UO_2)_4O(OH)_6(H_2O)_6$ lattice

(space group Pbca) with lattice parameters a = 16.728 Å, b = 14.700 Å, and c = 14.300 Å. The aggregate size was determined to be 20–30 nm. Although both XRD patterns exhibited the characteristic peaks of MOX, they exhibit slight differences. Quantifying the hydroxide content was challenging because the two hydroxide phases present within the MA-bearing MOX fuel powders—α-$UO_2(OH)_2$ and $(UO_2)_4O(OH)_6(H_2O)_6$ were partly amorphous. The lattice parameters of these hydroxides matched those of pure U hydroxides,[23,24] indicating that parts of U segregated as U hydroxides with no Pu contents. Although the mixed nitrate solution was heated at 750°C, the conversion to oxides remained incomplete. The presence of different hydroxides in the MA-bearing MOX fuel powders was confirmed. These differences may arise from slight variations in preparation conditions or from differences in the oxidation states of MA and residual FP. The denitration process of the U and Pu nitrate solutions is influenced by complex thermodynamics and kinetic factors. Optimizing the denitration conditions, such as heating time and temperature, is crucial for improving the conversion to oxides.

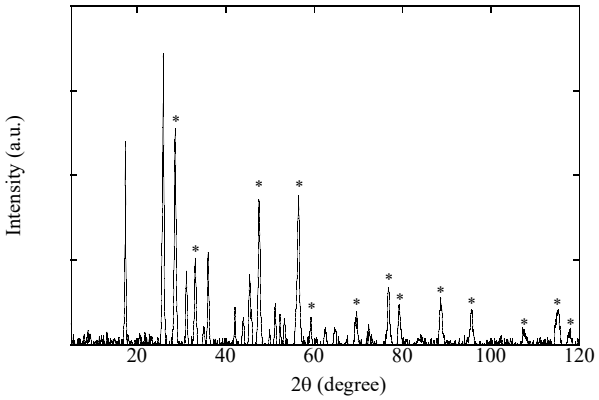

Fig. 3 XRD pattern of 2.3% MA-bearing MOX fuel powder. Asterisks (*) indicate the reflections of MOX.

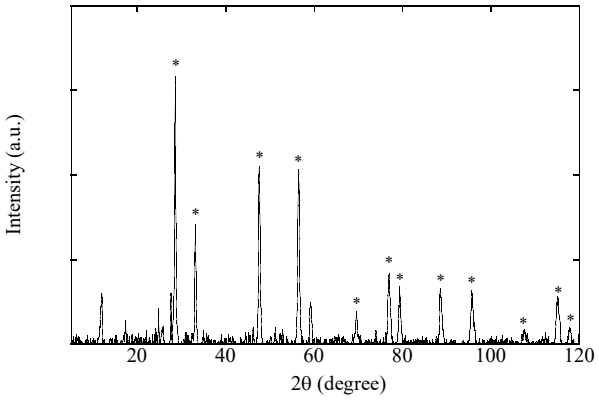

Fig. 4 XRD pattern of 6.8% MA-bearing MOX fuel powder. Asterisks (*) indicate the reflections of MOX.

Figure 5 shows the TG-DTA curves of 2.3% MA-bearing MOX fuel powder. **Figure 6** shows the TG-DTA curves of 6.8% MA-bearing MOX fuel powder. The TG-DTA curves of both MA-bearing MOX fuel powders exposed to an Ar atmosphere reveal weight loss between 0 and 700°C. The weight loss and changes in the DTA curves of both samples at around 100°C correspond to the vaporization of H_2O and the removal of impurities. Beyond 100°C, additional weight loss is observed. It is reported that α-$UO_2(OH)_2$ forms to UO_3 at 289–361°C, and UO_3 decomposes to U_3O_8 above 500°C.[25] The changes in the DTA curve of the 2.3% MA-bearing MOX fuel powder were observed at around 300 and 500°C. This suggests the potential decomposition of the α-$UO_2(OH)_2$ phase. Meanwhile, weight loss of 6.8% MA-bearing MOX fuel powders was observed at around 200°C. $(UO_2)_4O(OH)_6(H_2O)_6$ partially release H_2O molecule.[26] Some hydroxides in the 6.8% MA-bearing MOX fuel powders would release H_2O molecules and convert them to oxides. Further investigation is required to understand the oxidation behavior of the hydroxides fully.

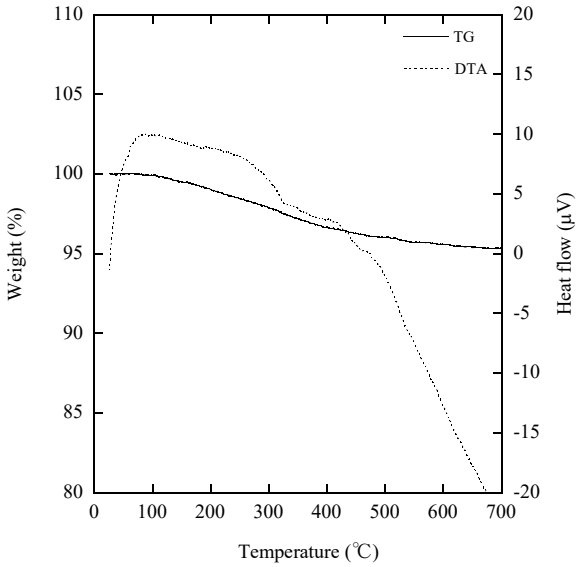

Fig. 5 TG-DTA curves of 2.3% MA-bearing MOX fuel powder.

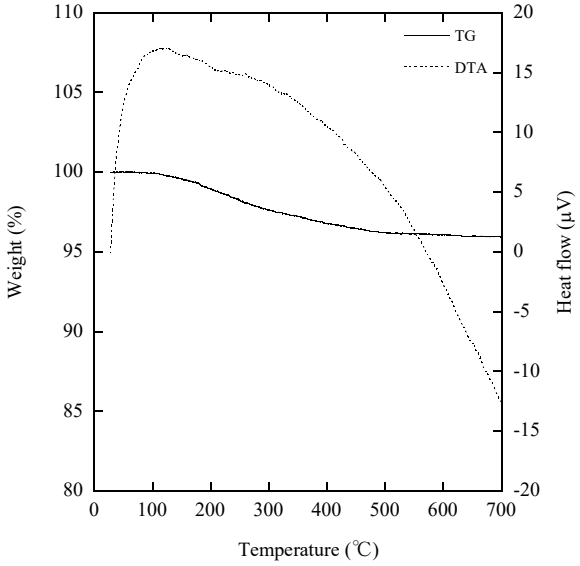

Fig. 6 TG-DTA curves of 6.8% MA-bearing MOX fuel powder.

IV. Conclusion

To recycle MA in the fast reactor fuel cycle, the preparation of feedstock for MA-bearing MOX fuel powder was studied. MA was separated from high-level liquid waste derived from irradiated fast reactor fuel using extraction chromatography. The recovered MA nitrate solution was mixed with the dissolver solution of MOX fuel, and MA-bearing MOX fuel powder was prepared using microwave heating. In addition to this powder, another MOX fuel powder was prepared without adding the MA nitrate solution. Both powders were characterized using XRD, and the measured XRD data were analyzed using DIFFRAC.TOPAS software. The XRD confirmed the presence of different hydroxides in both samples. In addition, the TG-DTA curves were measured to investigate the thermal characteristics. In summary, examinations of the denitration behavior and characteristics of MA-bearing MOX fuel powders provide valuable insights into their fabrication and irradiation behavior in the fast reactor fuel cycle.

Acknowledgment

This work was supported by the Ministry of Education, Culture, Sports, Science and Technology of Japan (MEXT) Innovative Nuclear Research and Development Program, Grant Number JPMXD0219214921. The authors express their gratitude to Dr. Miwa of the JAEA for their advice on the MA-bearing MOX fuel. Appreciation is also extended to Dr. Vauchy and Dr. Hirooka of the JAEA for their efforts in evaluating the XRD data of the MA-bearing MOX fuel powders.

References

1) P. Baron, S. M. Cornet, E. D. Collins, G. DeAngelis, G. Del Cul, Yu. Fedorov, J. P. Glantz, V. Ignatiev, T. Inoue, A. Khaperskaya, I. T. Kim, M. Kormilitsyn, T. Koyama, J. D. Law, H. S. Lee, K. Minato, Y. Morita, J. Uhlíř, D. Warin, R. J. Tayor, "A review of separation processes proposed for advanced fuel cycles based on technology readiness level assessments," *Prog. Nucl. Energy*, **117**, 103091 (2019).
2) N. Woolstenhulme, C. Baker, C. Jensen, D. Chapman, D. Imholte, N. Oldham, C. Hill, S. Snow, "Development of irradiation test devices for transient testing," *Nucl. Technol.*, **205**[10], 1251-1265 (2019).
3) H. Oshima, "Development of microwave heating method for co-conversion of plutonium-uranium nitrate to MOX powder," *J. Nucl. Sci. Technol.*, **26**[1], 161-166 (1989).
4) J. P. Cooch, "Meeting customer requirements in the Sellafield MOX plant," *Proc. TOPFUEL 2001 Int. Topical Meeting – Nuclear Fuel: Development to Meet the Challenge of a Changing Market*, Stockholm, Sweden, May 27-30, 2001, 2B-3 (2001). [CD-ROM]
5) F. Lebreton, D. Prieur, A. Jankowiak, M. Tribet, C. Leorier, T. Delahaye, L. Donnet, P. Dehaudt, "Fabrication and characterization of americium, neptunium and curium bearing MOX fuels obtained by powder metallurgy process," *J. Nucl. Mater.*, **420**[1-3], 213-217 (2012).
6) F. Lebreton, D. Prieur, D. Horlait, T. Delahaye, A. Jankowiak, C. Léorier, F. Jorion, E. Gavilan, F. Desmoulière, "Recent progress on minor-actinide-bearing oxide fuel fabrication at CEA Marcoule," *J. Nucl. Mater.*, **438**[1-3], 99-107 (2013).
7) S. Hirooka, T. Matsumoto, M. Kato, T. Sunaoshi, H. Uno, T. Yamada, "Oxygen potential measurement of (U,Pu,Am)$O_{2\pm x}$ and (U,Pu,Am,Np)$O_{2\pm x}$," *J. Nucl. Mater.*, **542**, 152424 (2020).
8) K. Maeda, S. Sasaki, M. Kato, Y. Kihara, "Radial redistribution of actinides in irradiated FR-MOX fuels," *J. Nucl. Mater.*, **389**[1], 78-84 (2009).
9) M. Kato, K. Maeda, T. Ozawa, M. Kashimura, Y. Kihara, "Physical properties and irradiation behavior analysis of Np- and Am-bearing MOX fuels," *J. Nucl. Sci. Technol.*, **48**[4], 646-653 (2011).
10) D. Frazer, F. Cappia, J. M. Harp, P. G. Medvedev, K. J. McClellan, S. L. Voit, J. Giglio, D. Jädernäs, P. Hosemann, "Post-irradiation characterization of a high burnup mixed oxide fuel rod with minor actinides," *J. Nucl. Mater.*, **562**, 153545 (2022).
11) M. Nakahara, Y. Sano, K. Nomura, M. Takeuchi, "Partitioning of plutonium by acid split method with dissolver solution derived from irradiated fast reactor fuel with high concentration of plutonium," *J. Chem. Eng. Jpn.*, **51**[3], 237-242 (2018).
12) E. P. Horwitz, D. G. Kalina, H. Diamond, G. F. Vandegrift, W. W. Schulz, "The TRUEX process – A process for the extraction of the transuranic elements from nitric acid wastes utilizing modified PUREX solvent," *Solvent Extr. Ion Exch.*, **3**[1-2], 75-109 (1985).
13) V. N. Kosyakov, E. A. Yerin, "Separation of transuranium and rare-earth elements by extraction with HDEHP from DTPA solutions," *J. Radioanal. Chem.*, **43**[1], 37-51 (1978).
14) B. T. M. Willis, "Crystallographic studies of anion-excess uranium oxides," *J. Chem. Soc., Faraday Trans. 2*, **83**[7], 1073-1081 (1987).
15) V. J. Tennery, T. G. Godfrey, "Oxidation properties of (U,Pu)O_2 solid solutions," *J. Am. Ceram. Soc.*, **56**[3], 129-133 (1973).
16) R. J. McEachern, "A review of kinetic data on the rate of U_3O_7 formation on UO_2," *J. Nucl. Mater.*, **245**[2-3], 238-247 (1997).
17) C. Berthinier, C. Rado, C. Chatillon, F. Hodaj, "Thermodynamic assessment of oxygen diffusion in non-stoichiometric $UO_{2\pm x}$ from experimental data and Frenkel pair modeling," *J. Nucl. Mater.*, **433**[1-3], 265-286 (2013).
18) T. L. Markin, R. S. Street, "The uranium–plutonium–oxygen ternary phase diagram," *J. Inorg. Nucl. Chem.*, **29**[9], 2265-2280 (1967).
19) W. Van Lierde, J. Pelsmaekers, A. Lecocq-Robert, "On the phase limits of U_4O_9," *J. Nucl. Mater*., **37**[3], 276-285 (1970).
20) B. Belbeoch, C. Piekarski, P. Pério, "Structure of U_4O_9," *Acta Crystallogr.*, **14**[8], 837-843 (1961).
21) S. Hirooka, M. Kato, T. Tamura, A. T. Nelson, K. J. McClellan, K. Suzuki, "Oxidation and reduction behaviors of plutonium and uranium mixed oxide powders," *Proc. Int. Conf. Fast Reactors and Related Fuel Cycles: Safe Technologies and Sustainable Scenarios (FR-13)*, Paris, France, Mar. 4-7, 2013, IAEA-CN-199-148 (2013). [USB Flash Drive]
22) M. Kato, K. Konashi, N. Nakae, "Analysis of oxygen potential of $(U_{0.7}Pu_{0.3})O_{2\pm x}$ and $(U_{0.8}Pu_{0.2})O_{2\pm x}$ based on point defect chemistry," *J. Nucl. Mater.*, **389**[1], 164-169 (2009).
23) J. C. Taylor, "Structure of the α form of uranyl hydroxide," *Acta Crystallogr. B*, **27**[6], 1088-1091 (1971).
24) J. Plášil, "The crystal structure of uranyl-oxide mineral schoepite, $[(UO_2)_4O(OH)_6](H_2O)_6$, revisited," *J. Geosci.*, **63**[1], 65-73 (2018).
25) O. V. Nipruk, A. V. Knyazev, G. N. Chernorukov, Yu. P. Pykhova, "Synthesis and study of hydrated uranium(VI) oxides,

$UO_3 \cdot nH_2O$," *Radiochem.*, **53**[2], 146-150 (2011).
26) N. B. A. Thompson, V. L. Frankland, J. W. G. Bright, D. Read, M. R. Gilbert, M. C. Stennett, N. C. Hyatt, "The thermal decomposition of studtite: analysis of the amorphous phase," *J. Radioanal. Nucl. Chem.*, **327**[3], 1335-1347 (2021).